

Electronic Bubble States in Liquid Helium*

W. Beall Fowler

Department of Physics, Lehigh University, Bethlehem, Pennsylvania

and

D. L. Dexter

University of Rochester, Rochester, New York

(Received 7 June 1968)

A calculation of the optical properties of electronic bubbles in liquid helium is presented. Making use of the measured well depth and surface tension, we have computed the electronic states as a function of bubble size and have calculated the configuration coordinate diagrams, transition energies, oscillator strengths, lifetimes, cross sections, line shapes, linewidths, and estimated the magnitude of the static Jahn-Teller effect in an excited state. The dependence on pressure is considered for some of these quantities from 0–20 atm.

I. INTRODUCTION

Among the many fascinating properties of liquid helium¹ are those associated with charged imperfections. Following studies of positrons² and ions³ in this medium, considerable attention has been devoted recently to phenomena related to injected and trapped electrons.^{4–8} The central remarkable fact with which we shall be concerned is that the lowest energy state of an excess electron in liquid helium may be characterized as a particle in a box, a spherical cavity from which about a thousand He atoms are expelled.

The experimental facts which lead to this conclusion are (1) liquid He has a negative electron affinity (i. e., a barrier) of about one eV^{8,4}; (2) the photo-ionization spectrum,⁶ which is sensitive to bubble size, indicates a radius of about 20 Å.⁹ Theoretical ideas which make this conclusion palatable are based on (1) the Pauli principle, which gives rise to a strong He–electron repulsion; and (2) the low polarizability of He, which results in only a very weak attraction.^{10,11}

We adopt this picture of electrons in bubbles in the present paper and discuss the model in detail in Sec. II. In Secs. III–V, making use of the known density, surface tension, and well depth, we compute the energies, configuration coordinate diagrams, oscillator strengths, lifetimes, linewidths and line shapes, and absorption cross sections for some of the electronic states and transitions of interest. In Sec. VI the static Jahn-Teller effect is treated in an approximation which is indicative of the magnitudes to be expected. In Sec. VII we discuss the problem of the surface tension. In the final section, we consider some experimental implications of our results.

II. THE MODEL

We treat an electronic bubble in liquid He as if it were an electron bound in a spherical square-well potential. Calculations reported below justify the assumption that there is a single electron; no evidence to the contrary has been reported. Several experimental^{6,7} and theoretical¹⁰ works, including this one, indicate that the bubble radius is much larger than atomic dimensions, and one would expect to be able to ignore surface irregularities,

that is, to retain the concepts of surface tension and surface energy, except for modifications as discussed in Sec. VII. Calculations reported in Ref. 10 indicate no significant change in rounding off the edges of the potential, so we employ a step function for simplicity. The well depth V_0 is chosen to be 1.02 eV as determined in Ref. 4, consistent with the photo-ionization measurements of Ref. 6. We select a temperature of 1.3°K to agree with Ref. 6, and use the appropriate (macroscopic) surface tension $\sigma = 0.36$ erg/cm² at that temperature.¹³ The equilibrium vapor pressure at 1.3°K is only $P_0 = 1.2$ mm Hg,¹⁴ and the resulting P_0V term in the energy is negligible in comparison with the surface energy at bubble radii of interest. We shall present additional results for high applied pressure, however, where the PV term and σ are both significantly larger.

Other parameters of at least implicit importance are the low dielectric constant (the index of refraction is 1.0285 at 5462 Å¹⁵) and the atomic density (2.2×10^{22} cm⁻³¹⁶).

The wave functions of the bound electron extend somewhat into the liquid, of course, where they are modulated near each He atom by the requirement of orthogonality, thus producing the well. We ignore this modulation in the computation of transition matrix elements, since it is the same in both electronic wave functions.

III. ELECTRONIC STATES

According to our model, we seek the solutions of

$$\left(-\frac{\hbar^2}{2m}\nabla^2 + V\right)\psi_n(r) = \epsilon_n(R)\psi_n(r),$$

$$V = -V_0, \quad r < R \quad (1)$$

$$= 0, \quad r > R,$$

a problem treated in elementary textbooks on quantum mechanics.¹⁷ To the electronic energy $\epsilon_n(R)$, we add the surface energy $4\pi\sigma R^2$ and volume energy $\frac{4}{3}\pi PR^3$, to obtain the total E_n as a function of R . The polarization energy is ignored, following the arguments of Ref. 10. Only spherical distortions are considered here. The effect of $l=2$ modes on the linewidth is considered in Sec. IV, and the ef-

fect of nonspherical distortions when the system is in a p state is considered in Sec. VI.

The calculations were carried out on a CDC-6600 computer at New York University, using a routine written by Herman and Skillman,¹⁸ modified by Smith (Illinois), and further modified by Kunz (Lehigh). Certain points were also evaluated by hand from the analytic solutions¹⁷ as a check of the numerical method.

The resulting plots of $E_n(R)$ versus R are noteworthy in the history of the theory of imperfections in condensed matter in that they depict reasonably accurate calculations of a "center" on a one-dimensional "configurational coordinate" diagram. Figure 1, for example, computed with $P=0$, predicts that the equilibrium radius is about 17.5 Å (which is between the experimental values deduced in Refs. 6 and 7), and that the $1s-1p$ oscillator strength should be 0.97; a $1s-2p$ transition should occur at 0.49 eV with oscillator strength 0.025, and no further bound optical transitions should occur. Furthermore (see Sec. IV) we can readily predict the absorption linewidths and line shapes. This center is much simpler than those encountered in solids, and this model itself is probably better than the vastly more difficult models required by other centers.

The usual Stokes shift is exhibited in Fig. 1; that is, after the system at equilibrium at 17.5 Å is excited to a p state by absorption of a photon, the medium would relax to a new minimum energy configuration, here represented as still spherical, and emission would occur at lower energy. For example, the $1s-1p$ transition would occur at 0.11 eV, and the corresponding $1p-1s$ energy would be 0.075 eV. (It should be recalled that transitions occur vertically on diagrams of this sort. Usually it is because of the Franck-Condon principle, which tells us that if they do not occur this way, there

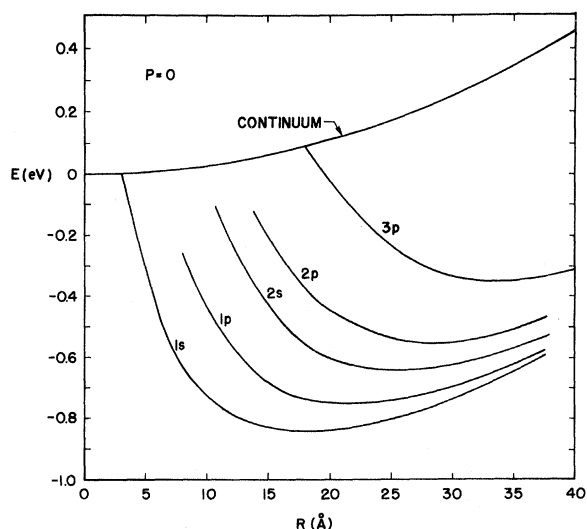


FIG. 1. Configuration coordinate diagram for an electronic bubble in liquid He with a well depth 1.02 eV, surface tension $\sigma=0.36$ erg cm⁻², and zero pressure.

will be diminution of the transition matrix element because of cancellation in the vibrational overlap integrals. In our case, a nonvertical transition would imply a shrinkage or expansion of the bubble in the unrealistically short time of $\sim 10^{-14}$ sec.)

Normalized radial wave functions computed at points of interest in Fig. 1 are presented in Fig. 2. The solid (dashed) curves represent the wave functions for the $1s$ and $1p$ states evaluated at the $1s(1p)$ minimum.

Along with total energies, we have also computed oscillator strengths, absorption cross sections, and lifetimes, and thus we can predict (for a spherical bubble) absorption and emission energies and transition probabilities.

Key numerical results are shown in Table I. The equilibrium radii listed there should be regarded as uncertain to perhaps $\frac{1}{2}$ Å, since the curves are rather flat and these radii were obtained from the curves.

Several results should be emphasized from Fig. 1 and Table 1. First, the oscillator strength into the $1p$ state is very large, 0.97, corresponding to a cross section of 1.0×10^{-16} eV cm². In fact, less than 0.005 is left for the $3p$ state plus continuum (a cross section $< 5 \times 10^{-19}$ eV cm²). It is just this low strength which was observed in the photo-ionization experiment, testimony to the sensitivity of the technique.

It should be noted that the oscillator strengths for the $1s-p$ transitions are close to those for $p-1s$, in the absence of the Jahn-Teller effect, in spite of a sizable (40%) change in the squared dipole matrix element. The energy change almost cancels that in the squared matrix element, even with large distortion. Such a result was not obviously to be expected.¹⁹

The $3p$ state at radii below about 19.5 Å is degenerate with the continuum. This suggests that absorption into this region of $3p$ may lead to auto-ionization. This possibility was noted⁶ in connec-

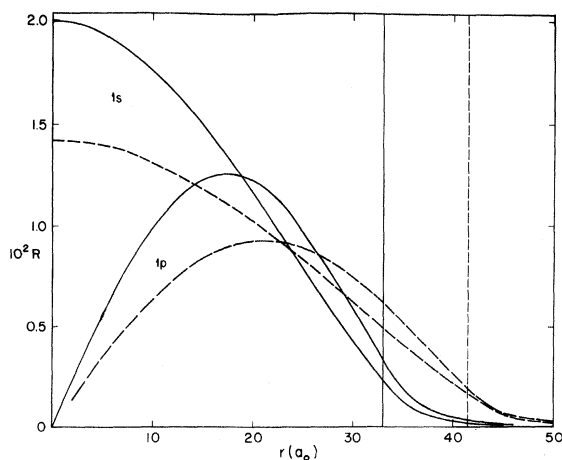


FIG. 2. Radial wave functions for the $1s$ and $1p$ states evaluated at 17.5 Å bubble radius (solid curves) and 22.5 Å (dashed curves). The vertical lines correspond to the two radii.

TABLE I. Computed absorption and emission parameters for the spherical electron bubble with $P=0$.

Equil. radius (Å)	Transition	E (eV)	Oscillator strength	Lifetime (sec)
Absorption				
17.5	$1s \rightarrow 1p$	0.11	0.97	...
17.5	$1s \rightarrow 2p$	0.49	0.025	...
17.5	$1s \rightarrow 3p$	0.96	< 0.005 (in continuum)	...
17.5	$1s \rightarrow \text{continuum}$	0.92	< 0.005	...
Emission				
22.5	$1p \rightarrow 1s$	0.075	...	1.27×10^{-5}
27.5	$2p \rightarrow 1s$	0.22	...	5.5×10^{-5}
35.0	$3p \rightarrow 1s$	0.30	...	1.55×10^{-4}

tion with one of the peaks observed in the photo-ionization experiment.

Predicted radiative lifetimes of the excited p states are rather long, 10^{-4} – 10^{-5} sec. Such long lifetimes raise the possibility that a bubble excited into $2p$ or $3p$ will not emit from that state, but will rather execute a radiationless decay and emit from a lower state, e.g., $1p$, or be trapped metastably in, e.g., $2s$ or $1d$. This possibility can best be explored experimentally.

As has been pointed out by others,^{10,20} the application of external pressure is expected to cause significant changes in the equilibrium bubble radius and in transition energies. There has been some discussion in the literature of the pressure-dependence of the surface tension, and the matter still seems rather unsettled (see Sec. VII). We have assumed that σ varies with P according to the Amit-Gross theory,²¹ starting at 0.36 erg cm^{-2} at $P=0$; at 1, 10, and 20 atm, then, σ is taken to be 0.37, 0.50, and 0.62 erg cm^{-2} , respectively.

We have computed the configuration coordinate curves for several different pressures, and in Fig. 3 and Table II shows some of the results. Note, for example, that in going from 0 to 20 atm the $1s$ bubble radius decreases from 17.5 to 11.0 Å, the $1s \rightarrow 1p$ transition energy increases from 0.11 to 0.24 eV, and the $1s \rightarrow \text{continuum}$ transition energy decreases from 0.92 to 0.79 eV. The 20-atm bubble radius of 11 Å is close to the experimental value of 10.22 Å obtained by Springett and Donnelly⁷ at that pressure.

It would be of interest to study the properties of the bubble at even higher pressures, especially pressures at which helium solidifies.

IV. VIBRATION FREQUENCIES AND LINEWIDTHS

An expression for the vibrational frequency of a liquid drop surrounded by a different liquid was first derived by Rayleigh.²² Setting the density of the inner liquid to zero (corresponding to a bubble), one obtains the result

$$\omega^2 = (l+1)(l-1)(l+2)\sigma/\rho R_0^3, \quad (2)$$

where l is the angular momentum quantum number

of oscillation, σ is the surface tension, ρ is the density of the liquid, and R_0 is the equilibrium radius of the bubble. This expression is not applicable for $l=0$, since liquid drops are (approximately) incompressible. (We present below our derivation for the breathing-mode frequency.) The Rayleigh result for $l=2$ also does not precisely describe our case, since it applies to an empty bubble and not to one containing an electron. However, it is of interest to use Eq. (2) to estimate the frequency of the $l=2$ mode. Using $\sigma=0.36 \text{ erg cm}^{-2}$, $\rho=0.145 \text{ g cm}^{-3}$, and $R_0=17.5 \text{ Å}$, we obtain $\hbar\omega=5 \times 10^{-5} \text{ eV}$.

For the breathing mode, we let R be the radius of the bubble and ρ be the density. The kinetic energy of a shell of fluid at radius r of thickness dr is equal to

$$dT = \frac{1}{2} \rho 4\pi r^2 dr \dot{r}^2. \quad (3)$$

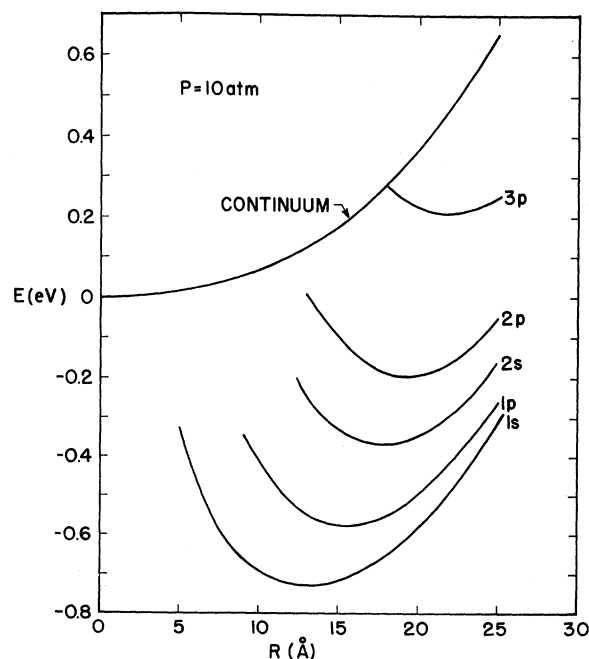


FIG. 3. The same as Fig. 1, but with a pressure of 10 atm and $\sigma=0.50 \text{ erg cm}^{-2}$, as discussed in the text.

TABLE II. Transition energies as a function of pressure. See Table I for zero-pressure results.

Pressure (atm)	Equil. radius (Å)	Transition	ΔE (eV)
1	17.0	Absorption $1s \rightarrow 1p$	0.12
1	17.0	$1s \rightarrow 2p$	0.52
1	17.0	$1s \rightarrow 3p$	(in continuum)
1	17.0	$1s \rightarrow$ continuum	0.93
1	21.0	Emission $1p \rightarrow 1s$	0.09
1	26.5	$2p \rightarrow 1s$	0.25
1	31.0	$3p \rightarrow 1s$	0.39
10	13.0	Absorption $1s \rightarrow 1p$	0.18
10	13.0	$1s \rightarrow 2p$	0.73
10	13.0	$1s \rightarrow 3p$	(in continuum)
10	13.0	$1s \rightarrow$ continuum	0.85
10	15.5	Emission $1p \rightarrow 1s$	0.13
10	19.5	$2p \rightarrow 1s$	0.40
10	21.5	$3p \rightarrow 1s$	0.73
20	11.0	Absorption $1s \rightarrow 1p$	0.24
20	11.0	$1s \rightarrow 2p$	(in continuum)
20	11.0	$1s \rightarrow$ continuum	0.79
20	14.0	Emission $1p \rightarrow 1s$	0.16

We assume the fluid to be incompressible, which means that an increase of bubble radius by an amount dR is related to an increase dr of the shell radius r through the expression

$$\frac{4}{3}\pi[(R_0 + dR)^3 - R_0^3] = \frac{4}{3}\pi[(r + dr)^3 - r^3], \quad (4)$$

$$\text{or } R_0^2 dR = r^2 dr. \quad (5)$$

Thus we obtain

$$\dot{r}^2 = (R_0^4/r^4)\dot{R}^2 \quad (6)$$

$$\text{and } dT = \frac{1}{2}\rho 4\pi R_0^4 \dot{R}^2 dr/r^2. \quad (7)$$

Integrating, we find

$$T = \frac{1}{2}\rho 4\pi R_0^3 \dot{R}^2 = \frac{1}{2}\rho 4\pi R_0^3 \delta^2, \quad (8)$$

where $R = R_0 + \delta$ defines the displacement from equilibrium δ . We now use a potential energy of the form

$$V = V_0 + b\delta^2, \quad (9)$$

where b will be obtained from the configuration coordinate curve, Fig. 1. Assuming harmonic oscillation and using the Lagrange equations, we obtain

$$\omega^2 = b/2\pi\rho R_0^3. \quad (10)$$

Using (from Fig. 1) $b = 1.02 \times 10^{-3}$ eV Å⁻², $\rho = 0.145$ g cm⁻³, and $R_0 = 17.5$ Å, we obtain $\hbar\omega = 3.8 \times 10^{-5}$ eV. Thus the breathing-mode frequency is lower than and rather close to the estimated $l=2$ frequency (5×10^{-5} eV/ \hbar).

Gross and Tung-Li²³ have computed the vibrational frequencies for the bubble plus electron, assuming an infinite potential well for the electron. They found that the frequency of the $l=2$ mode is $\pi/2^{1/2}$ times that of the $l=0$ mode. During preparation of this manuscript, we received a preprint by

Celli *et al.*²⁴ containing a similar calculation.

To obtain the predicted line shapes and linewidths, we employ classical configuration coordinate theory.²⁵

It is easily verified that the vibrational quantum state reached in the optical transition is a highly excited one; hence we expect the absorption and emission lines to be approximately Gaussian in shape. The widths are computed from geometrical considerations, and the absorption width at half-maximum is given by

$$W_A(T) = 2K_e X_0 \left(\frac{1.386}{K_g} \frac{\hbar\omega_g}{2} \coth \frac{\hbar\omega_g}{2kT} \right)^{1/2}, \quad (11)$$

where ω_g is the pertinent vibrational frequency, K_g and K_e are force constants for ground and excited states, respectively, and X_0 is the displacement of the minimum of the excited state from that of the ground state.

For the contribution of breathing-mode ($l=0$) vibrations to the width of the $1s \rightarrow 1p$ transition, we use $X_0 = 5.0$ Å, $K_e = 1.78 \times 10^{-3}$ eV Å⁻², $K_g =$ twice the value of b given above, and ω_g , the value given above for the breathing mode. We obtain a contribution of breathing modes to the $T=0^\circ\text{K}$ half-width of 0.001 eV. Since all the excited states appear to have about the same curvature, the main variable will be X_0 , and we expect the contribution of breathing modes to the $1s \rightarrow 3p$ width to be about 0.003 eV. At 1.3°K the coth function increases from unity to 5.8, so the $l=0$ contribution to the $1s \rightarrow 1p$ line-width increases to 0.0025 eV and that to the $1s \rightarrow 3p$ width to 0.008 eV. It is remarkable that because of the low vibrational frequency the line broadening is already approaching the high temperature $T^{1/2}$ limit at 1.3°K, and the linewidth is therefore to a good approximation independent of ω_g . Thus any spread of frequency in the small l modes due to interaction with phonons is not expected materially to affect the linewidth.

We have also estimated the contribution of $l=2$ vibrations to the width of the $1s-1p$ transition. For this calculation, we used a force constant K_g (actually, $K_g/5$, by virtue of its definition) and vibrational frequency ω_g given in Ref. 24. In a linear approximation, $K_e X_0$ is equal to minus the rate of change of excited-state energy with respect to vibrational coordinate; this, in turn, can be related to a derivative of energy with respect to eccentricity e as defined by Feenberg and Ham-mack.²⁶ We find, then, using the relation between eccentricity and coordinate given by Moszkowski,²⁷ that $K_e X_0$ in Eq. (11) should be replaced by $(3/2R_0) \partial E / \partial e$. We used the expression derived in Ref. 26 for the energy as a function of eccentricity to compute $\partial E / \partial e$; the result, for the contribution of $l=2$ modes to the linewidth of the $1s-1p$ transition at 1.3°K is about 0.01 eV. If we again assume (with-out as firm evidence this time) that the $1s-3p$ width will be about 3 times as large as that of $1s-1p$, we predict that the contribution of $l=2$ modes to the $1s-3p$ half-width will be about 0.03 eV.

This is to be compared with a half-width of approximately 0.04 eV, observed⁶ for the photo-conductivity signal tentatively attributed to a $1s-3p$ transition. Configuration interaction of the excited state with the continuum could easily account for some of the broadening of this transition.

It thus appears that the $l=2$ mode will be about 4 times as effective as the $l=0$ mode in broadening the optical transitions. This result is rather surprising, in view of the case of the F center in alkali halides, in which the breathing mode is generally at least as important as the other modes. However, in the present case, the rate of change of energy with eccentricity seems to be very large for small e ; in fact, this rate of change, if extrapolated to large e , would yield a static Jahn-Teller effect (see Sec. VI) several times as large as computed by better means.

V. THE STABILITY OF TWO ELECTRONS IN A SINGLE BUBBLE

We briefly mention the result of a calculation in which we estimated the energy of two electrons in a bubble. We used a variational technique with hydrogenic wave functions to compute the electronic energy, as in an elementary treatment of the atomic helium problem.¹⁷ We found that although such a system forms a bound state with respect to two free electrons and no bubble, the system would be unstable (by about 1 eV) against decay into two separated bubbles, each with one electron. In other words, the Coulomb repulsion of the electrons is too great for two of them to exist stably in a single bubble.

VI. THE STATIC JAHN-TELLER EFFECT

The static Jahn-Teller effect has been widely discussed in the color center and molecular literature,²⁸ but is extremely difficult to treat quantitatively in condensed matter. It appears that this effect might well be large in the bound p states of this system. It seems a logical assumption that

the sphere would tend to deform into a prolate spheroid, with the long axis parallel to the axis of the p function. This intuitive feeling is reinforced by the consideration that the p function has no probability density along the equator, and hence benefits little from the well in this region; thus it could afford to shrink the cavity at the equator and expand along the poles with no increase in surface energy. Performing an exact calculation for a particle in a finite spheroidal potential is a non-trivial task. However, there are perturbation variational techniques available for an approximate solution of the problem if the deviation from a known sphere is not too great.^{26,27} To obtain an idea as to the magnitude of the deviation to be expected we computed the "exact" results for a model which, while less appealing physically, allows an estimate of the Jahn-Teller distortion to be made. In this model, we constrained the bubble to the shape of a rectangular parallelepiped, and used harmonic oscillator wave functions in a variational approach to compute the distortion. Then in the most general case four parameters had to be varied, two for the box size and two to describe the wave functions. This was done with a computer routine, which we ran on a GE-225 computer at Lehigh.

Results of this calculation are shown in Table III. The most significant results are these: The static Jahn-Teller effect depresses by about 0.03 eV the energy of the $1p$ state whose axis is parallel to the long dimension of the parallelepiped, and the box is distorted a good deal, going from a cube of edge length 34 Å to a parallelepiped with edge lengths 24.4, 24.4, and 49.8 Å. One should also note that the edge length of a cube whose surface area equals that of a sphere of radius 17.5 Å (appropriate to the $1s$ state) is 25.4 Å; this is not far from the edge length of 27.6 Å computed. The variational principle, of course, prevents the energies in the parallelepiped model from being as low as the exact values.

The energy reduction of 0.03 eV in passing from the cube to the parallelepiped in the $1p$ state is a large fraction (40%) of the $1p-1s$ emission energy (0.075 eV) predicted in Sec. III, and of course the distortion is great also, with an axial ratio greater than 2. Presumably the energy of the $1s$ state in an ellipsoidal bubble will be raised by a comparable amount, shifting the emission band to perhaps 0.03 eV. It seems doubtful that approximate methods will suffice for treating such large distortions with quantitative reliability, and we shall

TABLE III. Rectangular parallelepiped model for the electron bubble. $V_0=1.02$ eV and $\sigma=0.35$ erg cm⁻². Results refer to the equilibrium position for each state. X , Y , and Z are the edge lengths of the parallelepiped.

State	Energy (eV)	X, Y (Å)	Z (Å)
$1s$	-0.788	27.6	27.6
$1p$ (no JT)	-0.687	33.9	33.9
$1p$ (JT)	-0.718	24.4	49.8

defer further discussion of this point.

During the preparation of this manuscript a paper appeared²⁹ in which, *inter alia*, an estimate of the bubble deformation is presented. This is a variational calculation with infinite well depth, and shows a reduction of 0.021 eV in the energy of the p_z state in a prolate ellipsoid as compared with a sphere. This paper called our attention to a brief note³⁰ in which an infinite well depth and radius 19 Å were assumed. Some results are presented dealing with the $1s \rightarrow 1p$ transition, and both papers treat Raman scattering.

VII. THE SURFACE TENSION

In the preceding calculations, we used a value of surface tension at zero pressure of $\sigma = 0.36$ erg cm^{-2} and considered the pressure variation to be according to the Amit-Gross theory.²¹ 0.36 erg cm^{-2} corresponds to the bulk surface tension measured by Atkins and Narahara¹³ at 1.3°K. In point of fact, there seems to be great uncertainty as to what the surface tension of the helium bubble is and how it varies with radius, pressure, and temperature. This difficulty has been discussed by several authors, and we merely review briefly their arguments.

One of the earliest treatments of the surface tension of bubbles or liquid drops was the thermodynamical approach of Tolman,³¹ extended by Kirkwood and Buff,³² and discussed by Hirschfelder *et al.*³³ This theory is formulated in terms of a distance parameter z_0 , and it is found that for a constant z_0 the surface tension *decreases* from the planar value as the radius of curvature decreases. Unfortunately, calculation of z_0 requires a detailed knowledge of the radial distribution function and the density distribution near the surface. Briscoe *et al.*¹² have suggested that z_0 for the helium bubble may be 3.5 Å. In the absence of firm estimates we have ignored the correction, but it might be noted in passing that the addition of 3.5 Å to our computed $1s$ radius would bring it into close agreement with what we believe to be the "best" experimental value, 21 Å of Ref. 6.

A more recent calculation of surface tension at zero pressure was that of Reiss *et al.*³⁴ They assumed a radius-dependent surface tension of the form proposed by Tolman, and computed the relevant parameters by a statistical-mechanical calculation of the energy expended on the introduction of a spherical cavity into a classical rigid-sphere fluid. In the limit of infinite radius, the results of their theory may be compared with experiment, and Reiss *et al.* found that whereas for many liquids the agreement is satisfactory, for helium at 4.2°K the theory predicts a value of the surface tension more than twice as large as that measured; furthermore, as T goes to zero, the surface tension is predicted to go to zero. Using their theory for the Tolman correction, one obtains a value of z_0 equal to 0.8 Å for the conditions specified in Sec. II. It has been pointed out by Springett *et al.*²⁰ that this theory is not applicable in the low-temperature region, because it predicts σ to be proportional to T .

Hiroike *et al.*³⁵ have presented a calculation of

the surface tension in which they used the formal similarity between the pair distribution function of a boson system with a wave function expressed as the product of pair wave functions and the pair distribution function of a classical fluid. They computed a surface tension of 0.52 erg cm^{-2} , and found that the surface tension varies approximately as the square of the density.

Amit and Gross²¹ computed the 0°K surface tension at a planar surface using a Hartree approximation, assuming a δ -function pseudopotential for the helium-helium interaction. They obtained

$$\sigma = 0.7\hbar C\rho, \quad (12)$$

where ρ is the density and C is the velocity of first sound.

Finally, Springett *et al.*²⁰ developed several approaches, one of which combined the experimental results of Springett and Donnelly on the pressure dependence of R with the predictions of the Wigner-Seitz model for the electronic states. They found a variation of σ with pressure similar to that predicted by Amit and Gross,²¹ although the absolute values of σ which they preferred were larger.

In view of these disagreements and uncertainties in the surface tension, we have somewhat arbitrarily chosen to use the experimental value appropriate to $T = 1.3^\circ\text{K}$ and equilibrium vapor pressure, and have used the Amit-Gross theory to predict the pressure-dependence. The semiempirical approach of Springett *et al.*²⁰ has attractions, but the disagreement between various experimentalists regarding the zero-pressure bubble radius (for example, Springett and Donnelly⁷ deduce a value of 16 Å, while the work of Northby and Sanders⁶ indicates 21 Å) leaves some uncertainty in this procedure.

VIII. CONCLUSIONS

We have computed various optical properties to be expected for electronic bubbles in liquid He. In particular, we predict an intense Gaussian absorption line at 0.11 eV at low pressure, with a width, W_A , of 0.01 eV at 1.3°K. The integrated absorption cross section Σ of 1.0×10^{-16} eV cm^2 implies a maximum absorption coefficient of

$$\mu_{\max} = \frac{N\Sigma}{W_A} \left(\frac{4}{\pi \ln 2} \right)^{1/2} = 1.35 \times 10^{-14} N, \quad (13)$$

where N is the bubble concentration in cm^{-3} and μ_{\max} is in cm^{-1} .

Measurement of the absorption should be feasible for $N = 10^{11} \text{cm}^{-3}$, or substantially less with modern (e.g. phase-sensitive) techniques. We understand that to the present time much smaller concentrations have been present in electrical investigations,³⁶ but it does not seem impossible to increase the concentration to $\gtrsim 10^{10} \text{cm}^{-3}$.

In studies of luminescence it is commonly found that photo-excitation spectra are readily measurable when absorption is impossible to detect. The photoconductivity experiment of Northby and Sanders⁶ is a closely related case. It should be em-

phasized in connection with photo-excitation of luminescence that the oscillator strength for $1s-1p$ excitation is 200 times the total to the continuum, so that the high sensitivity of electrical measurements is partly compensated for by the increased absorption in the lower-energy range. Excitation in the 0.1-eV region should produce $1p-1s$ luminescence at $\lesssim \frac{1}{2}$ the energy, and should be a valuable tool for investigating both the absorption curve and the Jahn-Teller effect.

It should be noted that a static electric field during the excitation experiment should give rise to polarized emission. A field of 10^8 V/cm applied along a 60-Å long spheroidal bubble should com-

pletely orient the relaxed excited bubbles [$(10^8 \text{ eV/cm}) 60 \times 10^{-8} \text{ cm} = 6 \times 10^{-4} \text{ eV}$; kT at 1.3°K is $1.1 \times 10^{-4} \text{ eV}$], and radiation should be detectable only perpendicular to the applied field. Other fields may well be useful, of course, as in electro-absorption measurements.

The luminescence properties of the bubbles are not predicted here with much reliability, both because of the Jahn-Teller effect and because of possible nonradiative internal conversion during relaxation. If the bubbles *do* luminesce, however, a valuable means for investigating their structure is at hand.

* Research supported in part by Grants Nos. AF-AFOSR 1276-67 and 611-67 from the U. S. Air Force Office of Scientific Research.

¹J. Wilks, The Properties of Liquid and Solid Helium (Oxford University Press, New York, 1967).

²R. A. Ferrell, Phys. Rev. **108**, 167 (1957).

³F. Reif and L. Meyer, Phys. Rev. **119**, 1164 (1960).

⁴M. A. Wolf and G. W. Rayfield, Phys. Rev. Letters **15**, 235 (1965).

⁵J. Levine and T. M. Sanders, Phys. Rev. Letters **8**, 159 (1962).

⁶J. A. Northby and T. M. Sanders, Phys. Rev. Letters **18**, 1184 (1967).

⁷B. E. Springett and R. J. Donnelly, Phys. Rev. Letters **17**, 364 (1966).

⁸W. T. Sommer, Phys. Rev. Letters **12**, 271 (1964).

⁹There is additional corroborative evidence. See particularly Ref. 7.

¹⁰J. Jortner, N. R. Kestner, S. A. Rice, and M. H. Cohen, J. Chem. Phys. **43**, 2614 (1965).

¹¹In this connection it should be noted that when the electron is replaced by a (neutral) positronium atom, so that the attractive polarization energy is reduced, bubble formation also occurs in liquid Ne, Ar, and H₂. See Ref. 12.

¹²C. V. Briscoe, S.-I. Choi, and A. T. Stewart, Phys. Rev. Letters **20**, 493 (1968).

¹³K. R. Atkins and Y. Narahara, Phys. Rev. **138**, A437 (1965).

¹⁴H. Van Dijk and M. Durieux, Physica **24**, 920 (1958).

¹⁵M. H. Edwards, Can. J. Phys. **36**, 884 (1958).

¹⁶E. C. Kerr, J. Chem. Phys. **26**, 511 (1957).

¹⁷See, for example, L.I. Schiff, Quantum Mechanics, (McGraw-Hill Book Company, Inc., New York, 1955), 2nd ed.

¹⁸F. Herman and S. Skillman, Atomic Structure Calculations (Prentice-Hall, Inc., Englewood Cliffs, New Jersey, 1963).

¹⁹W. Beall Fowler and D. L. Dexter, Phys. Rev. **128**, 2154 (1962).

²⁰B. E. Springett, M. H. Cohen, and J. Jortner, Phys. Rev. **159**, 183 (1967).

²¹D. Amit and E. P. Gross, Phys. Rev. **145**, 130 (1966).

²²Quoted by H. Lamb, Hydrodynamics, (Cambridge University Press, Cambridge, England, 1924), pp. 448-450, 5th ed.

²³E. P. Gross and H. Tung-Li, Phys. Rev. **170**, 190 (1968).

²⁴V. Celli, M.H. Cohen, and M. J. Zuckermann, Phys. Rev. **173**, 253 (1968).

²⁵C. C. Klick and J. H. Schulman, in Solid State Physics, edited by F. Seitz and D. Turnbull (Academic Press, Inc., New York, 1957), Vol. 5.

²⁶E. Feenberg and K. C. Hammack, Phys. Rev. **81**, 285 (1951).

²⁷S. A. Moszkowski, Phys. Rev. **99**, 803 (1955).

²⁸See, e.g., R. S. Knox and A. Gold, Symmetry in the Solid State (W. A. Benjamin, Inc., New York, 1964).

²⁹B. Duvall and V. Celli, Phys. Letters **26A**, 524 (1968).

³⁰I. A. Fomin, Zh. Eksperim i Teor. Fiz. Pis'ma Redakt. **6**, 715 (1967) [English transl.: JETP Letters **6**, 196 (1967)].

³¹R. C. Tolman, J. Chem. Phys. **17**, 333 (1949).

³²J. G. Kirkwood and F. P. Buff, J. Chem. Phys. **17**, 338 (1949); F. P. Buff and J. G. Kirkwood, ibid. **18**, 991 (1950); F. P. Buff, ibid. **19**, 1591 (1951).

³³J. O. Hirschfelder, C. F. Curtiss, and R. B. Bird, Molecular Theory of Gases and Liquids (John Wiley & Sons, Inc., New York, 1954), p. 348.

³⁴H. Reiss, H. L. Frisch, E. Helfand, and J. L. Lebowitz, J. Chem. Phys. **32**, 119 (1960).

³⁵K. Hiroike, N. R. Kestner, S. A. Rice, and J. Jortner, J. Chem. Phys. **43**, 2625 (1965).

³⁶See, however, G. E. Spangler and F. L. Hereford, Phys. Rev. Letters **20**, 1229 (1968).